Chapter 6

MAS NMR investigation of self-assembled zinc chlorin dyes for artificial light-harvesters

MAS NMR spectroscopy has been employed to investigate the self-assembly of two zinc chlorin dyes. The semi-synthetic zinc chlorins, derived from naturally occurring chlorophyll *a*, differ only in their 3^1 substituents with one having a hydroxy group and the other a methoxy both of which can self-assemble into chromophore stacks in the solid state. Using the ^1H-^{13}C heteronuclear dipolar correlation MAS NMR experiment on natural abundance samples, a ^1H chemical shift assignment of the chlorin ring of the hydroxy-chlorin and methoxy-chlorin was made and corresponding aggregation shifts relative to their monomer shifts in solution were determined. DFT ring-current shift calculations revealed unambiguously that out of two possible types of well-ordered π-stacked arrangements of the aggregates that have been observed for the methoxy-chlorin in solution, *i.e.* the parallel stack and the antiparallel stack, in the solid-state both zinc chlorins self-assemble in antiparallel stacks. X-ray diffraction data available for the methoxy-chlorin have provided validation of its antiparallel structure and reveal a unit cell with Zn-Zn distances of 6.2 Å, which is in good agreement with the Zn-Zn distance of 6.4 Å obtained from modeled aggregates of antiparallel stacks that are optimized with molecular mechanics. We have shown that even without isotopic enrichment or access to distance-constraints, access to the proton chemical shifts of aggregated zinc chlorins allows accurate probing of ring-currents and can be related to the stacking of macrocycles.

6.1 Introduction

Chlorosomal light harvesting systems are natural self-assembled BChl assemblies that are highly ordered, facilitating ultrafast inter-pigment excitation transfer [1]. In addition they have the longest exciton diffusion lengths of any known pigment assembly [2-4]. The extremely fast exciton mobility leads to favorable light-harvesting efficiencies of these systems, which recommend these aggregates for possible applications in supramolecular photonic, electronic or photocatalytic devices [5,6]. It is known that the self-assembly of BChl *c* pigments observed in chlorosomes is replicated by BChl *c* aggregates in non-polar solvents like hexane [7]. This phenomenon implies that the non-covalent interactions of the metal-3^1-OH coordination, π-π overlap between stacks, and 3^1-OH-13^1=O hydrogen bonding that binds the stacks together and provides the exciton delocalization pathway, are reproduced in the artificially aggregated BChl *c* systems.

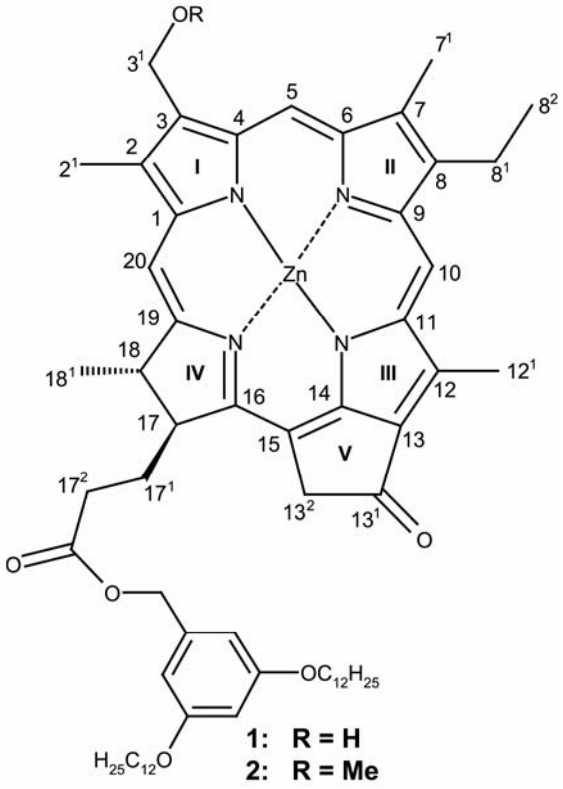

Figure 6.1 Chemical structure of 3^1-hydroxy and 3^1-methoxy zinc chlorins **1** and **2**.

To arrive at a better understanding of chlorosomal light-harvesting systems, Tamiaki and co-workers developed a model zinc chlorin compound which is a BChl *d* analogue that forms extended dye aggregates and replicates the aggregation behavior of BChl *c* in non-polar solvents [8]. In recent years, it has been demonstrated by Würthner and co-workers that the self-assembly process of BChl *c*, *d*, and *e* can be mimicked by using semi-synthetic molecules that are pre-programmed for self-assembly (Figure 6.1) [9-11]. These zinc chlorins can be prepared with various 17^2-substituents, by stepwise derivatization of Chl *a*. The aggregation of the newly synthesized compounds is completely reversible and triggered by a variation in solvent polarity. This favorable property allowed thorough spectroscopic and microscopic investigations for the elucidation of the aggregate structural features.

One of the newly synthesized compounds, **1**, also possesses the three functional units relevant for self-assembly found in the natural BChl counterpart, namely, the 3^1-OH group, a central metal ion, and 13^1C=O moieties along the Q_y axis and self-assembles into extended aggregates [9]. AFM investigations allowed the visualization of rod aggregate structures on a HOPG surface for zinc chlorin **1**, with resemblance to the nanorods of the natural chlorosomal self-assemblies [9]. This was considered an important step towards validation of the suitability of the zinc chlorin dyes for the imitation of chlorosomal antennae systems, and helps to pave the way for the preparation of biomimetic systems with superior light harvesting properties similar to the chlorosomal antennae [9,11].

In compound **2** the hydroxy functionality at 3^1 is replaced by a methoxy functionality in order to eliminate the H-bonding interaction of 3^1-OH-13^1=O that is thought to be involved in holdings stacks together (Figure 6.1). It was reported that compound **2** self-assembles as independent single-antiparallel or double-parallel stacks when aggregating from a non-polar solvent [10]. Depending on the concentration of the aggregate solutions, extended lamellae of single or double stack aggregates are formed on the HOPG surface that was used for the AFM and STM studies [10]. In addition to the suprastructure, the investigation of the packing mode of compound **2** in the solid-state is of importance considering the

potential use of such π stacks and layered-assemblies as bulk material in nanocircuits for supramolecular electronics.

In recent years, MAS NMR techniques have been successfully developed and used for structure determination of uniformly enriched compounds or multiple spin clusters in solid type biological systems. In particular, MAS methods have been applied successfully to ^{13}C and ^{15}N enriched samples to study the self-organisation of BChls in chlorosomal light harvesting antennae, as is demonstrated in Chapters 4 and 5 [12]. While labeling of biological systems is rapidly becoming routine, isotope enrichment of artificial systems is more difficult. First, a large fraction of labeled material is lost in a multi-step synthesis or derivatization process, and second, materials research critically depends on the preparation and screening of multiple compounds for realizing artificial systems with the desired properties. Scrutinizing every step in a supramolecular chemical design process with a laborious and lengthy, multi-step structure determination effort is highly impractical. In this chapter it is shown for compounds **1** and **2** how determination of structure can be achieved for unlabeled samples, based on chemical shift assignments and DFT calculations, and without access to distance-constraints. This is possible since the building blocks **1** and **2** are moderately sized, unsaturated molecules of low symmetry. The unsaturation leads to a favourable dispersion of NMR signals and resolved ^{1}H-^{13}C cross peaks in heteronuclear correlation spectra, while the low symmetry promotes a good accuracy of the DFT ring current analyses, since side chains are in unique positions in terms of overlap with adjacent molecules in the structure, allowing for the correlation of ring current effects with the underlying chemical structure.

To resolve the structural arrangement of the model systems using MAS NMR combined with molecular modeling and ring current shift calculations for unlabelled zinc chlorin dyes **1** and **2,** the ^{1}H shifts are first resolved using 2D heteronuclear ^{1}H-^{13}C dipolar correlation experiments and thereby the proton aggregation shifts are determined. Access to the proton chemical shifts of aggregated zinc chlorins allows accurate probing of ring-current effects that can be related to the stacking of macrocycles, via the chemical structure of the molecule. Quantum mechanical

calculations are then performed in order to quantitatively reproduce the observed ring currents. In this way, the combination of MAS NMR, molecular modeling and DFT based ring current shift calculations provides a quantitative basis to determine the stacking patterns that zinc chlorins **1** and **2** adopt at a molecular level.

6.2 Experimental section

Zinc chlorins **1** and **2** were derivatized and synthesized starting from Chl *a*, which was extracted from *Spirulina Platensis* cyanobacteria according to previously described methods [9-11,13,14]. The compounds were characterized by ^{1}H NMR and HRMS. ^{1}H NMR solution spectra were recorded at 25 °C with a 400 MHz spectrometer from Bruker GmbH, Ettlingen (Bruker Avance 400). The chemical shifts are given in reference to TMS or the residual solvent signals in ppm of the NMR frequency.

To prepare aggregates for the solid-state NMR measurements, the purified dyes **1** and **2** were dissolved in a minimum amount of THF and dichloromethane, respectively, and about 10 equiv. of n-hexane was added to each in order to form the aggregates in solution. The aggregates were precipitated at 0 °C, and solvents were removed under vacuum with a rotary evaporator. Subsequent to the removal of solvent, the solids were lyophilized for 2-3 days to transform them into a free-flowing powder which could be packed tightly in the NMR rotor. Spinning frequencies of 13 kHz ± 5 Hz and sample temperatures of 298 K were used for the 2D ^{1}H-^{13}C FSLG heteronuclear correlation experiments [15,16]. The ^{1}H spins were decoupled during acquisition using TPPM scheme [17]. For each of 256 steps in the indirect ^{1}H dimension, 1536 ^{13}C scans were accumulated, yielding a total measurement time of ~ 6 days to obtain adequate signal to noise for the assignment of the signals from the unlabeled compounds. The DFT based ring-current shift calculations were performed as described in Chapter 4 [18-25].

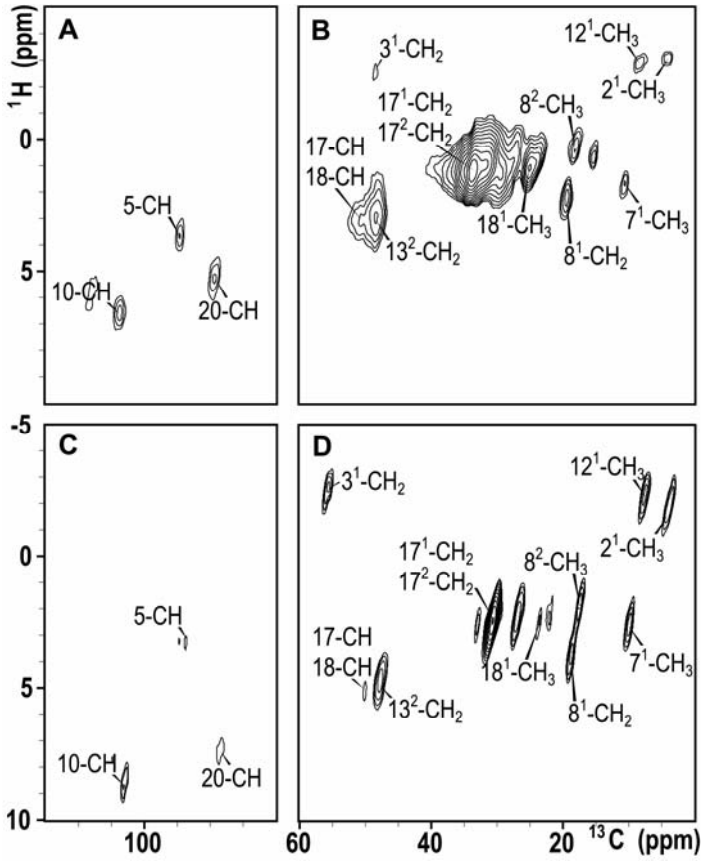

Figure 6.2 Contour plot sections of heteronuclear ^{1}H-^{13}C MAS NMR FSLG dipolar correlation spectra of zinc chlorins **1** (panels A and B) and **2** (panels C and D) recorded in a field of 17.6 T employing a spinning rate of 13 kHz and sample temperatures of 298K. The assignments of the correlations from the chlorin rings are indicated.

6.3 Results

For the assignment of the ^{1}H shifts, the FSLG technique was applied to solid samples of zinc chlorins **1** and **2** [16]. Figure 6.2 shows the 2D heteronuclear ^{1}H-^{13}C spectrum where the assignment is indicated. It was possible to assign almost all proton resonances corresponding to the chlorin ring unambiguously for compounds **1** and **2** as depicted in panels A-D in Figure 6.2. In addition, a single set of peaks is detected, which implies local crystalline order with the same structural environment for all molecules. The 3^1-OH and 3^1-OCH$_3$ resonances for zinc chlorins **1** and **2** were not observed, possibly because of some form of dynamics resulting in

excessive line broadening and inefficient CP. The solid state proton shifts are listed in Table 6.1 as $\sigma^H_{\mathbf{1},i}$ and $\sigma^H_{\mathbf{2},i}$ respectively [26].

Table 6.1 ^{1}H solution (σ^H_{liq}) and solid-state chemical shifts (σ^H_i) of zinc chlorins **1** and **2**, as well their aggregation shifts $\Delta\sigma^H_i = \sigma^H_i - \sigma^H_{liq}$ are given in ppm.

position	$\sigma^H_{\mathbf{1},i}$	$\sigma^H_{\mathbf{1},liq}$	$\Delta\sigma^H_{\mathbf{1},i}$	$\sigma^H_{\mathbf{2},i}$	$\sigma^H_{\mathbf{2},liq}$	$\Delta\sigma^H_{\mathbf{2},i}$
5	3.7	9.5	-5.8	3.3	9.3	-6.0
10	6.6	9.6	-3.0	8.8	9.6	-0.8
17	3.1	4.3	-1.2	5.1	4.2	0.9
18	3.1	4.5	-1.4	5.1	4.4	0.7
20	5.3	8.5	-3.2	7.4	8.4	-1.0
2^1	-3.1	3.3	-6.4	-1.8	3.3	-5.1
3^1	-2.5	5.7	-8.2	-2.6	5.6	-8.2
7^1	1.7	3.3	-1.6	2.6	3.3	-0.7
8^1	2.2	3.8	-1.6	3.8	3.7	0.1
8^2	0.4	1.7	-1.3	2.0	1.7	0.3
12^1	-2.9	3.7	-6.6	-2.3	3.7	-6.0
13^2	3.0	5.1	-2.1	4.7	5.1	-0.4
17^1	1.2	2.3	-1.1	2.4	1.9	0.5
17^2	1.2	2.3	-1.1	2.4	1.9	0.5
18^1	1.1	1.8	-0.7	2.4	1.7	0.7

Aggregation shifts are defined as chemical shifts in the solid relative to the monomer shifts in solution. To obtain these monomer shifts, zinc chlorin **1** was dissolved in coordinating solvents like THF-d_8 and zinc chlorin **2** was dissolved in pyridine-d_5. The ring current shifts that are observed in the chlorin aggregates relative to the monomers in solution provide invaluable information about the stacking of the molecules. In particular the ^{1}H shifts are an accurate probe of the secondary fields induced by the aromatic rings. The ^{1}H assignment was obtained from 1D ^{1}H NMR experiments. The ^{1}H monomer shifts for **1** and **2** are listed in Table 6.1 as $\sigma^H_{\mathbf{1},liq}$ and $\sigma^H_{\mathbf{2},liq}$, respectively. The aggregation shifts for **1** and **2** are calculated according to $\Delta\sigma^H_i = \sigma^H_i - \sigma^H_{liq}$ and are also listed in Table 6.1. Significant upfield aggregation shifts are observed, both for zinc chlorins **1** and **2**, and these have been depicted as circles for values less than -2 ppm in Figure 6.3, where the circles have a radius proportional to the magnitude of shift.

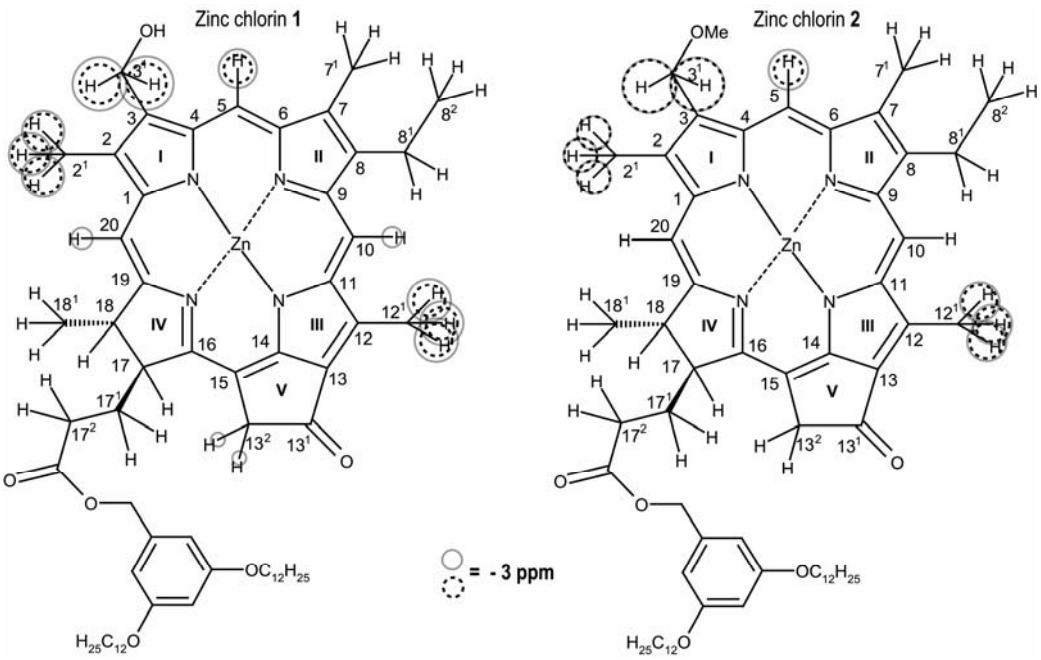

Figure 6.3 Detected ^{1}H upfield aggregation shifts of aggregated zinc chlorins **1** and **2** relative to their monomers in THF-d_8 and pyridine-d_5, respectively, are shown as solid grey circles. Calculated ring-current shifts for **1** and **2** in the antiparallel stack model are shown as dashed black circles. Values less than 2 ppm are depicted. The circles have a radius proportional to the magnitude of the shift.

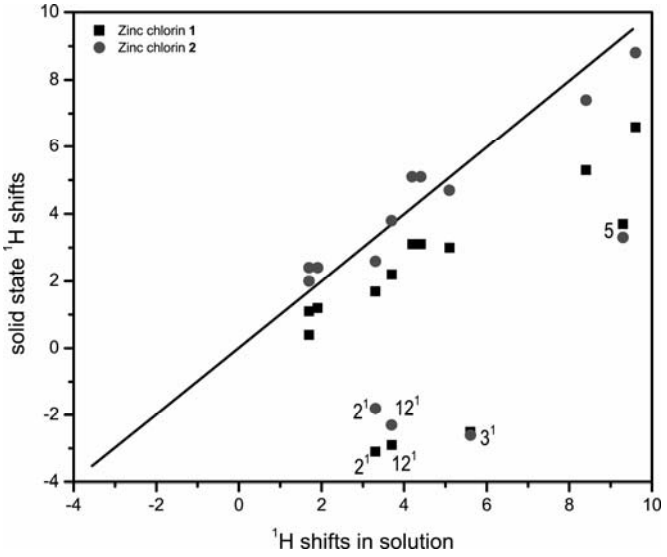

Figure 6.4 Chemical shift correlation plots for zinc chlorins **1** and **2**. The ^{1}H shifts in the solid samples **1** and **2** are plotted against the monomer shifts in THF-d_8 and pyridine-d_5 solution. The solid lines represent the diagonals. ^{1}H signals are indicated that show a large, upfield shift in the solid relative to the monomer in solution.

In addition, Figure 6.4 compares the solid state chemical shifts of **1** and **2** with their monomer shifts in solution. From the correlation plot it is clear how pronounced the ^{1}H aggregation shifts are within the ^{1}H chemical shift range. The ^{1}H aggregation shifts are very useful for structure determination since they are dominated by ring-current effects, in line with observations in other chlorin aggregates [26]. In particular the aggregation shifts for the ^{1}H signals that are far from the diagonal in Figure 6.4 are invaluable for structure determination. The magnitude of the aggregation shifts for zinc chlorins **1** and **2** (*cf*. Figure 6.3 and Table 6.1) are remarkably similar, which indicates that the pattern of stacking or the stacking motif is the same for both compounds in the solid state, despite a difference in the 3 side chain, OH with H-bonding capability for compound **1**, and a methoxy functionality for compound **2**.

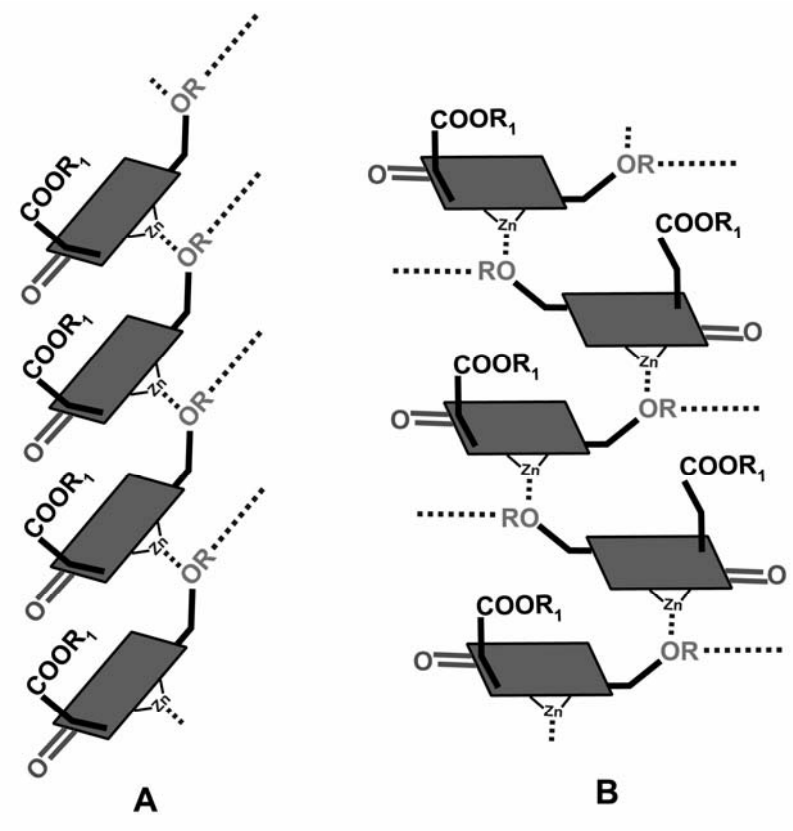

Figure 6.5 Schematic representation of the models used for ring-current shift calculations. (A) is the parallel-stack model and (B) is the antiparallel stack model. For zinc chlorin **1**, R=H and for **2**, R=Me. R_1 is the 3,5 dodecyloxybenzyl alcohol tail.

In order to explain the aggregation shift patterns, structural models of coordinating chlorins for **1** and **2** were considered based on stacking motifs observed in previously published AFM and STM data [9,10]. The first is the parallel stack model while the second is the antiparallel monomer stack model [27]. This is because compound **1** is shown to form rod like aggregates, which are thought to be built from the basic parallel stack motif [9]. Compound **2**, on the other hand, has been shown to aggregate with either the antiparallel stack motif or the parallel stack motif [10]. A schematic representation of these two models is given in Figure 6.5. To simplify the calculations, the tail has been replaced by a methyl group at 17- and the 8-ethyl is replaced by an 8-methyl group.

For zinc chlorins **1** and **2** a parallel stack model with five molecules each was constructed and optimized using molecular mechanics with the MM+ force field. The terminal chlorin was capped with a methanol molecule as the fifth ligand to prevent distortion. To investigate the possibility of H-bonding between stacks, larger aggregates of **1** were built by placing multiple stacks together with their 3^1-OH group of one stack within H-bonding distance of the 13^1=O of the adjacent stack followed by further MM+ optimization. In this way an additional twenty molecule aggregate of four pentamer stacks was optimized for zinc chlorin **1**. The inter-stack H-bond network remained intact on optimization. Due to the presence of the methoxy functionality at 3^1 in zinc chlorin **2**, H-bonding is not possible and only a single parallel stack comprising of ten zinc chlorin **2** molecules was optimized. This single parallel stack for compound **2** was energetically stable. To optimize the antiparallel stack model for **1** and **2**, an initial stack of five molecules was constructed for each of them. Geometry optimization revealed, however, that these structures are very unstable as single stacks. A second five molecule stack was added for both **1** and **2** in the inter-stack H-bonding arrangement for compound **1** and with the methoxy functionalities pointing towards the 13^1=O of the adjacent stack for compound **2**. On optimization, energetically stable aggregates were obtained for both compounds. This suggests that a charge stabilization mechanism is in operation in compound **2**, between the positive-like 3^1-OMe and the negative-like 13^1=O, which mimics the H-

bonding in compound **1**, and leads to an energetically favourable extended space filling structure. ^{1}H ring-current shifts were calculated for zinc chlorins **1** and **2** in the parallel and antiparallel stack models and are listed in Table 6.2.

Table 6.2 Calculated ring current shifts $\Delta\sigma^H_{calc}$ in (ppm) for zinc chlorins **1** and **2**, each in the parallel stack (P) and antiparallel stack (A) models. All values are in ppm.

position	$\Delta\sigma^H_{\mathbf{1},calc}$ (P)	$\Delta\sigma^H_{\mathbf{2},calc}$ (P)	$\Delta\sigma^H_{\mathbf{1},calc}$ (A)	$\Delta\sigma^H_{\mathbf{2},calc}$ (A)
5	-2.0	-1.8	-4.2	-4.3
10	-0.3	-0.2	1.5	0.3
17	2.1	-0.1	1.1	-0.2
18	1.3	-0.3	1.1	-0.1
20	-0.6	-0.1	0.7	-1.2
2^1	-2.9	-2.7	-5.5	-5.0
3^1	-3.7	-4.9	-6.0	-8.0
7^1	0.4	0.0	-0.7	-0.3
8^1	0.4	0.4	1.3	1.4
8^2	*a*	*a*	*a*	*a*
12^1	-3.3	-2.5	-4.8	-5.2
13^2	-0.5	-3.3	1.7	0.2
17^1	0.9	-0.1	1.6	-0.1
17^2	*b*	*b*	*b*	*b*
18^1	1.2	0.2	1.5	0.1

[a]Methyl group was used at C-8 to simplify optimization. [b]Tail was replaced by CH_3 at C-17 for ring-current shift calculation.

6.4 Discussion

From Tables 6.1 and 6.2, and Figure 6.3, it is clear that the aggregation shifts of zinc chlorin **2** are in good quantitative agreement with the calculated ring-current shifts for the antiparallel stack arrangement, rather than for the parallel stack arrangement, and they indicate a dense packing of the molecules in layers. On the other hand, the calculated ring-current shifts for **1** are in semi-quantitative agreement with the observed aggregation shifts for the antiparallel stack model though they reproduce the essential features, in particular the combination of very strong aggregation shifts in the 3-CH_2 region and significant 12-CH_3 shifts. In contrast, for the parallel stack model there are significant differences between the aggregation shifts and the DFT calculated ring-current shifts,

in particular for the 5-H, 10-H, 20-H, 2^1-H_3, 3^1-H_2, and 12^1-H_3 positions for compound **1** and the 5-H, 2^1-H_3, 3^1-H_2, and 12^1-H_3 positions for compound **2**. It is possible that the parallel stack like structure that is observed for both aggregates in solution, is energetically less likely in the solid state due to unfavorable electric dipole interactions.

The magnitude of the aggregation shift observed for the 12^1 protons for both compounds **1** and **2** precludes their existence as individual stacks in the solid-state. This is because in a single antiparallel stack there is no significant ring overlap in the region of 12^1-H_3 that could cause such a strong upfield shift (Table 6.1). Overlap with chlorins from adjacent stacks is thus essential. The tails constitute a factor that is important to the structure of the aggregates and is expected to affect the suprastructure of the aggregates. Zn chlorin **2** forms extensive lamellae of antiparallel stacks on atomically flat surfaces, as has been shown by the STM technique [10]. Our modeling indicates that single antiparallel stacks are energetically unstable. Probably the interdigitation of tails between adjoining stacks plays an important role in stabilizing the extended lamellar structure that is observed on surfaces, in contrast with the extended H-bonding in the natural BChl stacks.

X-ray powder diffraction data that is available for compound **2** shows non-equidistant reflections in the small and wide angle regions, which suggest a highly ordered three dimensional arrangement of the compound in the solid state [28]. It reveals a unit cell volume of 3.14 nm^3, which can be constituted of two molecules of zinc chlorin **2**, since after the increment system of Immirzi Perini, a molecule of chlorin **2** in the packing unit can have an estimated volume of 1.47 nm^3, which is approximately half the volume of the unit cell [29]. This suggests that the unit cell is made up of two molecules probably arranged in the antiparallel like fashion. The Zn-Zn distance from the optimized antiparallel aggregate of compound **2** is 6.4 Å, which is in very good agreement with a reflection, having a periodicity of 6.2 Å. Hence, there is converging evidence for a preferred antiparallel stacking arrangement in the solid state. Apparently with chlorin **2** there is inter-stack stabilization by charge pairing of 3^1 methoxy

and 13[1]=O keto functionalities in adjacent stacks that matches the role of H-bonding in chlorin **1** for stabilizing the 3-D space filling structure.

6.5 Conclusions

Synthetic zinc chlorins **1** and **2** were self-aggregated in hexane and cyclohexane respectively, and studied in detail to gain insight into their packing behavior in the solid-state. The specific aim of the work presented in this chapter is to resolve the self-assembly behavior of zinc chlorin dyes in the solid-state by means of an effective method that combines proton chemical shifts and DFT calculations. The experimental aggregation shifts of zinc chlorins **1** and **2** were well reproduced by ring-current shift calculations of the antiparallel stacking mode. The antiparallel model for **2** agrees very well with the X ray diffraction data, since the molecular volume 3.14 nm^3 that transpires from the X-ray corresponds to the formation of a unit cell that can accommodate two molecules arranged in the antiparallel fashion. In addition, the Zn-Zn distance of 6.4 Å calculated from modeling is in close agreement with the value of 6.2 Å obtained from the diffraction data.

Thus, in this chapter it has been shown how quantum mechanical calculations allow experimental ^1H solid-state NMR spectra to be assigned in a quantitative manner to a specific molecular packing arrangement, starting from the chemical structure of a moderately sized molecule with different side chains that break the molecular symmetry. This approach is based on marked sensitivity of ^1H chemical shifts to ring currents arising from nearby aromatic rings. There is no need for isotopic labelling for the heteronuclear MAS NMR experiments, and eventually the development of a model to account for the quantitative agreement of observed and experimental ring-current shift values is possible. The combination of heteronuclear MAS NMR experiments, molecular modeling and ring-current shift calculations provides a fingerprinting technique that can be of use in the future to investigate structure and properties of other unlabeled π aggregated supramolecular systems of low molecular symmetry.

References

[1] A. R. Holzwarth, M. G. Müller and K. Griebenow (**1990**) *Journal of Photochemistry and Photobiology B-Biology* 5: 457-465.

[2] D. C. Brune, G. H. King, A. Infosino, T. Steiner, M. L. W. Thewalt and R. E. Blankenship (**1987**) *Biochemistry* 26: 8652-8658.

[3] S. Savikhin, P. I. Vannoort, Y. W. Zhu, S. Lin, R. E. Blankenship and W. S. Struve (**1995**) *Chemical Physics* 194: 245-258.

[4] V. I. Prokhorenko, D. B. Steensgaard and A. R. Holzwarth (**2003**) *Biophysical Journal* 85: 3173-3186.

[5] H. Tamiaki, M. Amakawa, A. R. Holzwarth and K. Schaffner (**1995**), (P. Mathis, Eds.) Kluwer, Dordrecht.

[6] G. D. Scholes and G. Rumbles (**2006**) *Nature Materials* 5: 683-696.

[7] T. S. Balaban, A. R. Holzwarth, K. Schaffner, G. J. Boender and H. J. M. de Groot (**1995**) *Biochemistry* 34: 15259-15266.

[8] H. Tamiaki, A. R. Holzwarth and K. Schaffner (**1992**) *Journal of Photochemistry and Photobiology B-Biology* 15: 355-360.

[9] V. Huber, M. Katterle, M. Lysetska and F. Würthner (**2005**) *Angewandte Chemie-International Edition* 44: 3147-3151.

[10] V. Huber, M. Lysetska and F. Würthner (**2007**) *Small* 3: 1007-1014.

[11] V. Huber, S. Sengupta and F. Würthner (**2008**) *Chem. Eur. J.*

[12] B. J. van Rossum, D. B. Steensgaard, F. M. Mulder, G. J. Boender, K. Schaffner, A. R. Holzwarth and H. J. M. de Groot (**2001**) *Biochemistry* 40: 1587-1595.

[13] H. Tamiaki, M. Amakawa, Y. Shimono, R. Tanikaga, A. R. Holzwarth and K. Schaffner (**1996**) *Photochemistry and Photobiology* 63: 92-99.

[14] K. M. Smith, D. A. Goff and D. J. Simpson (**1985**) *Journal of the American Chemical Society* 107: 4946-4954.

[15] A. Bielecki, A. C. Kolbert and M. H. Levitt (**1989**) *Chemical Physics Letters* 155: 341-346.

[16] B. J. van Rossum, H. Forster and H. J. M. de Groot (**1997**) *Journal of Magnetic Resonance* 124: 516-519.

[17] A. E. Bennett, C. M. Rienstra, M. Auger, K. V. Lakshmi and R. G. Griffin (**1995**) *Journal of Chemical Physics* 103: 6951-6958.

[18] M. J. Frisch et al. (**2004**) Gaussian, Inc., Wallingford CT.

[19] A. D. Becke (**1986**) *Journal of Chemical Physics* 84: 4524-4529.

[20] C. T. Lee, W. T. Yang and R. G. Parr (**1988**) *Physical Review B* 37: 785-789.

[21] J. C. Facelli (**1998**) *Journal Of Physical Chemistry B* 102: 2111-2116.

[22] Z. F. Chen, C. S. Wannere, C. Corminboeuf, R. Puchta and P. V. Schleyer (**2005**) *Chemical Reviews* 105: 3842-3888.

[23] R. Ditchfield (**1972**) *Journal of Chemical Physics* 56: 5688-5691.

[24] K. Wolinski, J. F. Hinton and P. Pulay (**1990**) *Journal of the American Chemical Society* 112: 8251-8260.

[25] R. Ditchfield (**1974**) *Molecular Physics* 27: 789-807.

[26] I. de Boer et al. (**2004**) *Journal of Physical Chemistry B* 108: 16556-16566.

[27] A. R. Holzwarth and K. Schaffner (**1994**) *Photosynthesis Research* 41: 225-233.

[28] S. Ganapathy, S. Sengupta, P. K. Wawrzyniak, V. Huber, F. Buda, F. Würthner and H. J. M. de Groot: *In Preparation*

[29] A. Immirzi and B. Perini (**1977**) *Acta Crystallographica Section A* 33: 216-218.